

## PHOTODISINTEGRATION OF OXYGEN. I.

A. N. GORBUNOV and V. A. OSIPOVA

P. N. Lebedev Physics Institute, Academy of Sciences, U.S.S.R.

Submitted to JETP editor February 21, 1962

J. Exptl. Theoret. Phys. (U.S.S.R.) **43**, 40-50 (July, 1962)

The cross sections and angular distributions for the  $(\gamma, p)$  and  $(\gamma, n)$  reactions in oxygen were measured with a cloud chamber in a magnetic field. The integral photon absorption cross section was determined in the giant resonance region and up to 170 MeV. An asymmetry in the forward direction was found in the neutron angular distribution for the  $(\gamma, n)$  reaction. The results indicate that nucleon correlations in the nucleus play a significant role.

## 1. INTRODUCTION

GREAT interest in the experimental study of the photodisintegration of oxygen has arisen recently in connection with the theoretical investigations of the nuclear photon effect in double magic nuclei on the basis of the shell model.<sup>[1-3]</sup>

Many experimental studies<sup>[4-18]</sup> have been devoted to the photodisintegration of oxygen. In these studies, a large amount of data on the photoeffect in  $O^{16}$  has been obtained for excitation energies below 30 MeV. Several sharp peaks in the proton absorption cross section for oxygen nuclei have been found. The position of these peaks is in good agreement with the calculations of Elliot and Flowers.<sup>[1]</sup> However, according to other data,<sup>[17-19]</sup> the ratio of the integral cross sections corresponding to the main peaks at  $\sim 22$  and 25 MeV for the  $(\gamma, p)$  reactions turns out to be 1:2, while the theoretical ratio of the integral absorption cross sections for these excitation energies is 2:1. Moreover, there is no explanation for the breaks in the excitation curve for the  $O^{16}(\gamma, n)O^{15}$  reaction, the number of which considerably exceeds the number of electric dipole transitions allowed in the  $O^{16}$  nucleus by the shell model.

In connection with conclusions of the theory that the single-particle E1 transitions in  $O^{16}$  are localized at excitation energies below 30 MeV, it is of interest to carry out an experiment at higher excitation energies. In the present paper, the photoeffect in oxygen was investigated with a cloud chamber in a magnetic field operating in a bremsstrahlung beam of maximum energy  $E_{\gamma \max} = 170$  MeV.

## 2. EXPERIMENTAL METHOD

The experimental arrangement used in our experiment has been described in detail earlier.<sup>[20]</sup> A cloud chamber 30 cm in diameter and 8 cm high operated in a magnetic field of intensity  $\sim 10.5 \times 10^3$  Oe. The chamber was filled with oxygen in a mixture with water and alcohol vapors (in a ratio of 3:1 by volume) to a pressure of 265 mm Hg. With a mixture of this composition, the number of impurity nuclei (carbon) in the chamber was no greater than 4% of the number of oxygen nuclei. A reduced pressure was used to increase the range of the recoil nuclei produced in the  $(\gamma, p)$ ,  $(\gamma, n)$ , and  $(\gamma, pn)$  reactions and to decrease their scattering. The relative stopping power of the mixture (after the expansion of the chamber) was 0.29 for slow protons. With such a stopping power, the recoil nuclei produced in the  $(\gamma, p)$ ,  $(\gamma, n)$ , and  $(\gamma, pn)$  reactions have ranges up to 20 mm and are not scattered very strongly. This permits not only the identification of all these reactions (see<sup>[21]</sup>) but also the measurement of emission angles and the recoil-nuclei ranges.

The momenta and emission angles of the particles were measured in the following way. During the study of the  $(\gamma, p)$  reactions, we selected for measurement cases in which the projected length of the proton track on the plane of the chamber bottom was  $\geq 53$  mm. (With a depth of  $\sim 60-62$  mm for the illuminated region of the chamber, this condition corresponds to the selection of tracks with an angle of inclination  $\leq 30^\circ$  to the plane of the bottom of the chamber.) The projec-

tions of the proton angles of emission relative to the beam direction were determined from measurements on a UIM-21 microscope. The space angles were calculated from the plane angles by means of the relation

$$\theta = \arccos \frac{\cos \alpha}{\sqrt{1 + (h/l)^2}},$$

where  $\theta$  is the proton angle of emission relative to the beam,  $\alpha$  is its projection on the plane of the chamber bottom,  $2h$  is the depth of the illuminated region of the chamber,  $l$  is the projected length of the track. Under our conditions, the angles  $\theta$  and  $\alpha$  differed appreciably only for  $\alpha < 30^\circ$  and  $\alpha > 150^\circ$ . The angles of emission of the tracks in this region were measured with the aid of a reprojector which permitted the spatial reconstruction of the tracks by means of stereoscopic pictures.

The radii of curvature of the tracks in the magnetic field were determined by comparison of the track curvature with standard templates. For radii of curvature up to 200 cm, this method ensures rapid and sufficiently accurate measurements ( $\sim 3-5\%$ ). In the calculation of the proton momentum, we also took into account the momentum component parallel to the magnetic field.

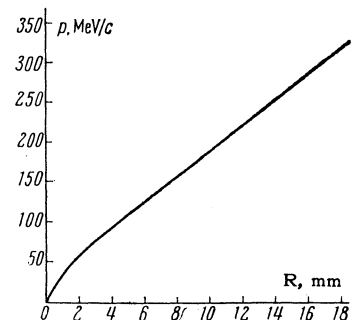
In connection with the fact that we selected for the measurements proton tracks with angles of inclination relative to the plane of the chamber no greater than  $30^\circ$ , we determined the total number of protons emitted at an angle  $\theta$  to the beam axis from the number of measured tracks by introducing the correction factor

$$k(\theta) = \pi/2 \arcsin \frac{1}{2 \sin \theta}.$$

In the study of the  $O^{16}(\gamma, n)O^{15}$  reaction, the emission angles of the  $O^{15}$  recoil nuclei relative to the beam axis and their ranges were measured with the aid of a reprojector. In most cases, the direction of an  $O^{15}$  track with range greater than 3 mm could be determined from the appreciable scattering at the end of its range and from the thinning-down of the track due to the decrease in the effective charge. The error in the measurement of the recoil nucleus range was 0.5 mm, the error in the angular measurement for tracks of range  $\sim 6-10$  mm did not exceed  $5^\circ$ .

In order to determine the momenta of the  $O^{15}$  recoil nuclei from their ranges, we used the range-energy relation shown in Fig. 1. This relation was found from the experimental range energy curve for  $N^{15}$  nuclei obtained by us from measurements of tracks produced in the  $O^{16}(\gamma, p)$

FIG. 1. Range-energy curve for  $O^{15}$  ( $R$  is the range of the recoil nucleus in the chamber gas).



$N^{15}$  reaction and from the ratio of the  $O^{15}$  and  $N^{15}$  momenta (of equal range) according to the data of Blackett and Lees.<sup>[22]</sup>

The method of measurement of the synchrotron radiation intensity has been described by us earlier.<sup>[20]</sup>

A total of 732 proton tracks from  $O^{16}(\gamma, p)N^{15}$  reactions and 1256  $O^{15}$  recoil-nucleus tracks from  $O^{16}(\gamma, n)O^{15}$  reactions was measured.

### 3. RESULTS OF THE MEASUREMENTS<sup>1)</sup>

A. Reaction Yields. The numbers of cases and the relative yields of different photonuclear reactions in oxygen recorded on 14,600 cloud chamber pictures (including 10,600 pictures with the magnetic field) are shown in Table I. As seen from the table, the  $(\gamma, p)$  and  $(\gamma, n)$  reactions are mainly photonuclear processes in oxygen. The ratio of their yields is

$$Y(\gamma, n)/Y(\gamma, p) = 0.60 \pm 0.024.$$

This ratio was found from a series of 4000 pictures taken without a magnetic field, for part ( $\sim 8\%$ ) of the  $O^{15}$  tracks emitted from the  $O^{16}(\gamma, n)O^{15}$  reactions could have been missed in the scanning, owing to the large background of slow electrons in the pictures with the magnetic field.

B. Cross sections for the  $(\gamma, p)$  and  $(\gamma, n)$  reactions. In order to calculate the cross sections for the  $(\gamma, p)$  and  $(\gamma, n)$  reactions, we plotted the results of the angle-of-emission and momentum measurements for protons [in the  $(\gamma, p)$  reaction] and for  $O^{15}$  nuclei [in the  $(\gamma, n)$  reaction] in a polar coordinate system in which the polar angle and radius vector were equal to the particle emission angle and momentum, respectively. Moreover, with the aid of a graphical method used in a previous experiment,<sup>[23]</sup> we calculated from these polar diagrams the cross sections for the  $O^{16}(\gamma, p)N^{15}$  and  $O^{16}(\gamma, n)O^{15}$  reactions under the assump-

<sup>1)</sup>See also [21].

Table I. Yields for various photonuclear reactions in oxygen

Type of Reaction	No. of observed events	Yield relative to ( $\gamma, p$ ) yield	Yield relative to total yield from all photonuclear reactions, %
( $\gamma, p$ )	4996	1	44.0
( $\gamma, n$ )	3004	0.60 $\pm$ 0.024	26.4
( $\gamma, pn$ )	1105	0.220 $\pm$ 0.007	9.7
( $\gamma, \alpha$ )	291	0.058 $\pm$ 0.004	2.6
( $\gamma, \alpha n$ )	204	0.041 $\pm$ 0.003	1.8
3-prong stars: total	1147	0.230 $\pm$ 0.008	10.1
( $\gamma, p\alpha$ )	383	0.077 $\pm$ 0.004	—
( $\gamma, p\alpha n$ )	99	0.020 $\pm$ 0.002	—
( $\gamma, 2p$ )	370	0.074 $\pm$ 0.004	—
( $\gamma, 2pn$ )	218	0.044 $\pm$ 0.003	—
( $\gamma, 2\alpha n$ )	11	0.002 $\pm$ 0.001	—
4-prong stars: total	402	0.080 $\pm$ 0.004	3.5
$\gamma, 4\alpha$	173	0.035 $\pm$ 0.003	—
$\gamma, 2\alpha pn$	136	0.027 $\pm$ 0.003	—
5-prong stars: total	189	0.038 $\pm$ 0.003	1.7
$\gamma, 2p 3\alpha 2n$	160	0.032 $\pm$ 0.003	—
6-prong stars: total	23	0.005 $\pm$ 0.001	0.2

tion that the final  $N^{15}$  and  $O^{15}$  nuclei are produced in the ground states. The cross sections obtained in this way are shown in Fig. 2. The arrows in the figures indicate the position of the two single-particle excited levels of the oxygen nucleus with  $J = 1^-$ ,  $T = 1$ , which, according to the calculations of Elliot and Flowers,<sup>[1]</sup> make the basic contribution to the electric dipole absorption of photons by oxygen nuclei.

C. Angular distribution of the ( $\gamma, p$ ) and ( $\gamma, n$ ) reaction products. Figure 3 shows the angular distributions of protons of energy  $> 0.5$  MeV emitted from ( $\gamma, p$ ) reactions. Figure 4 shows the angular distributions of the neutrons of energy  $E_n = 5-11$  MeV and  $E_n > 11$  MeV emitted in the ( $\gamma, n$ ) reaction.

The neutron energies and the angles of emission were determined from the emission angles and momenta of the  $O^{15}$  recoil nuclei with the aid of the conservation laws. It was assumed here that the final  $O^{15}$  nucleus is produced in its ground

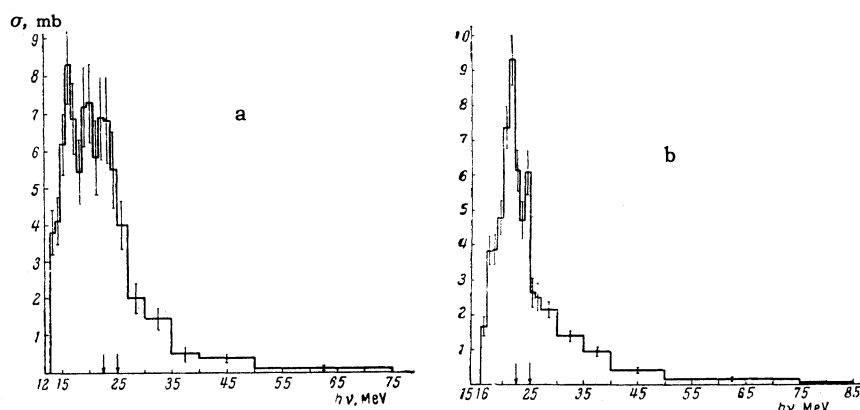
state. Of course, transitions in which the final nucleus remains in one of the excited states are also possible. Neglect of this possibility leads to errors in the calculated energy, momentum, and emission angle of the neutron. For neutrons of energy greater than 5 MeV, the error in the calculation of the emission angle is no greater than  $5^\circ$ , while the error in the energy is  $\sim 10\%$ .

In constructing the neutron angular distributions, we used only those cases of ( $\gamma, n$ ) reactions for which the direction of flight of the  $O^{15}$  recoil was rather reliably established from the characteristic scattering of the nucleus at the end of its range and from the thinning-down of the track. It is clear that the selection of cases for the construction of the angular distribution in this way cannot distort the shape of the angular distribution.

The angular distributions were approximated by the functions

$$f(\theta) = A + B \sin^2\theta$$

FIG. 2. a — cross section for the ( $\gamma, p$ ) reaction calculated under the assumption that  $N^{15}$  is produced in the ground state; b — cross section for the ( $\gamma, n$ ) reaction calculated under the assumption that  $O^{15}$  is produced in the ground state.



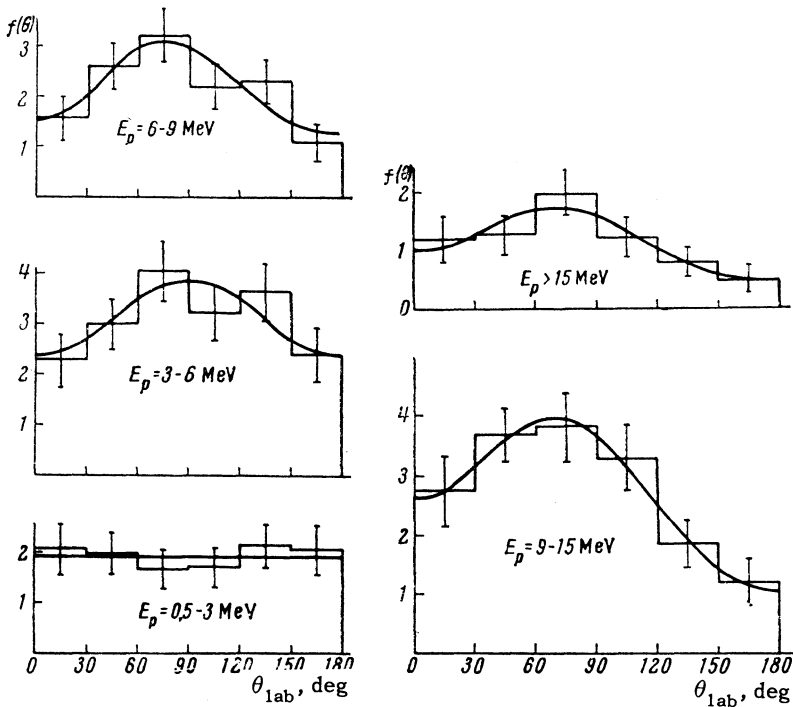


FIG. 3. Angular distributions of protons of different energies emitted in  $(\gamma, p)$  reactions.

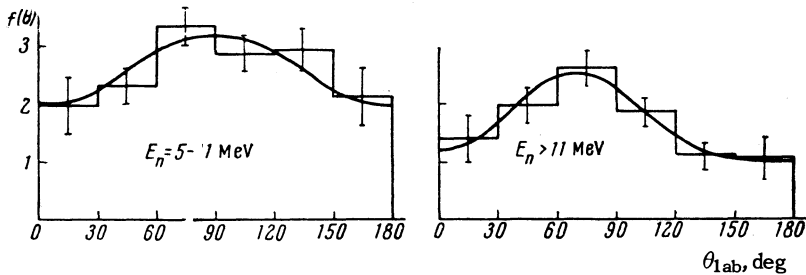


FIG. 4. Angular distributions of neutrons emitted in the  $(\gamma, n)$  reactions.

or

$$f(\theta) = A + B \sin^2 \theta + C \sin^2 \theta \cos \theta + D \cos \theta.$$

The first function corresponds to the nucleon angular distribution for the model of the direct photoeffect with pure electric dipole absorption. The second function takes into account the possibility of interference between the electric dipole absorption and the weak electric quadrupole and magnetic dipole absorption. The coefficients A, B, C, and D shown in Table II were found by the method of least squares.

#### 4. DISCUSSION OF RESULTS

##### 1. $(\gamma, p)$ and $(\gamma, n)$ reaction cross sections.

It is seen from Fig. 2a that the cross-section curve found for the  $(\gamma, p)$  reaction has peaks at 16.5, 20, and 23 MeV. The position of the last peak is in good agreement with the position of the peak (22.6 MeV) in the cross section for electric dipole absorption of photons by  $O^{16}$  nuclei calculated by Elliot and Flowers.<sup>[1]</sup>

The curve in Fig. 2a was compared with the  $O^{16}(\gamma, p_0)N^{15}$  reaction cross section for transitions to the ground state of the final  $N^{15}$  nucleus, calculated from the data<sup>[17,18]</sup> on the inverse reaction  $N^{15}(p, \gamma_0)O^{16}$ . The comparison shows that the peaks of our experimental curve at 16.5 and 20 MeV are associated with transitions to an excited state of the final  $N^{15}$  nucleus, while the peak at 23 MeV is associated with a transition to the ground state.

The peak at 16.5 MeV is apparently connected with transitions to an excited state of  $N^{15}$  with  $E^* = 6.3$  MeV accompanied by the absorption of a photon of energy  $\sim 23$  MeV. The large probability for such transitions follows directly from the Wilkinson model.<sup>[24]</sup> In fact, according to this model, the allowed transitions in the absorption of a photon are those with  $\Delta l = \pm 1$ ,  $\Delta j = \pm 1, 0$  in which no more than one particle of the nucleus changes its configuration. Hence, if a proton is emitted from the internal subshell ( $1p_{3/2}$ ) when a proton is absorbed, then a hole  $1p_{3/2}^{-1}$ , corresponding to the  $N^{15}$  first excited state with  $E^*$

Table II

Energy	A, $\frac{\mu b}{\text{sr-MeV-Q}}$	E/A	C/A	D/A
Protons from $O^{16}(\gamma, p)N^{15}$ reaction				
$E_p$				
0.5 - 3	30 $\pm$ 3			
3 - 6	30 $\pm$ 5	0.6 $\pm$ 0.4		
6 - 9	18 $\pm$ 4	1.2 $\pm$ 0.6	0.6 $\pm$ 0.8	0.1 $\pm$ 0.3
9 - 15	12 $\pm$ 2	1.0 $\pm$ 0.5	0.4 $\pm$ 0.6	0.4 $\pm$ 0.3
15 - 50	0.8 $\pm$ 0.25	1.2 $\pm$ 0.7	0.7 $\pm$ 1.1	0.4 $\pm$ 0.4
Neutrons from $O^{16}(\gamma, n)O^{15}$ reaction				
$E_n$				
5 - 11	15 $\pm$ 2.5	0.6 $\pm$ 0.3	—	—
11 - 50	0.9 $\pm$ 0.2	1.1 $\pm$ 0.6	1.1 $\pm$ 0.7	0.1 $\pm$ 0.3

= 6.3 MeV, is produced. The large probability for transitions to the  $N^{15}$  state with  $E^* = 6.3$  MeV has been observed earlier by Johansson and Forkman. [6]

The cross sections obtained for the  $O^{16}(\gamma, n)O^{15}$  reaction (Fig. 2b) has two peaks at 21.5 and 24.5 MeV, whose positions are quite close to the positions of the two basic peaks of the  $O^{16}$  photon absorption cross section calculated by Elliot and Flowers and are in satisfactory agreement with positions of the peaks according to the data of Milone and Rubbino. [15] Carver and Lokan [11] measured the cross section for the  $O^{16}(\gamma, n)O^{15}$  reaction by the activation method and observed that it increases very slowly from the threshold ( $\epsilon = 15.6$  MeV) to the excitation energy  $\sim 20$  MeV. Our experimental curve increases in this energy region much more rapidly. This difference should apparently be ascribed to transitions to the excited states of the final  $O^{15}$  nucleus upon the excitation of the  $O^{16}$  nucleus by photons of energy greater than 23 MeV. Comparison of Figs. 2a and 2b, however, shows that the probability of transitions to excited states of the final nucleus in the case of the  $(\gamma, n)$  reaction is considerably less than in the case of the  $(\gamma, p)$  reaction. This has been noted earlier by Milone and Rubbino, [15] who explain it by the higher threshold for the  $(\gamma, n)$  reaction.

From the cross sections for the  $(\gamma, p)$  and  $(\gamma, n)$  reactions (Fig. 2), we calculated the integral cross sections of these reactions (Table III). It should be noted that the integral cross sections are somewhat reduced, since they were obtained under the assumption that the final  $N^{15}$  and  $O^{15}$  nuclei are produced in the  $(\gamma, p)$  and  $(\gamma, n)$  reactions in the ground states. Allowance for transitions to the excited states of the final nuclei could increase the integral cross section by 10% approximately for the  $(\gamma, p)$  reaction and by 5% for the  $(\gamma, n)$  reaction. Also shown in this table are the integral cross sections  $\sigma_0 = Y/\eta(E)$  for these reactions estimated in [21] from their absolute yields:

$$Y = \int_0^{170} \sigma(E) \eta(E) dE$$

under the assumption that  $\tilde{E} = 2\epsilon$ , where  $\epsilon$  is the reaction threshold. If we take into account the correction connected with transitions to excited states, then both estimates of the integral cross section for the  $(\gamma, p)$  reaction are in satisfactory agreement with one another. The value of the integral cross section for the  $(\gamma, n)$  reaction given in [21] turns out to be somewhat overestimated.

The integral cross sections for the  $(\gamma, p)$  and  $(\gamma, n)$  reactions for energies up to 30 MeV ob-

Table III. Integral cross sections for the  $(\gamma, p)$  and  $(\gamma, n)$  reactions in oxygen (in MeV-mb)

Reaction	1			2			3
	$E_\gamma \leq 30$	$E_\gamma > 30$	$E_\gamma \leq 170$	$E_\gamma \leq 30$	$E_\gamma > 30$	$E_\gamma \leq 170$	$E_\gamma \leq 170$
$(\gamma, p)$	90	17	107	100	17	117	129
$(\gamma, n)$	60	21	81	65	21	86	105
<b>Total</b>	150	38	188	165	38	203	234

Note: 1 - calculated under the assumption that the final  $N^{15}$  and  $O^{15}$  nuclei are produced in the ground state; 2 - a correction has been introduced to take into account (qualitatively) transitions to excited states of  $N^{15}$  and  $O^{15}$ ; 3 - estimated in [21] from the absolute yields of the  $(\gamma, p)$  and  $(\gamma, n)$  reactions ( $E_\gamma$  is given in MeV).

tained with allowance for transitions to excited states of the final nuclei [Table III (2)] are in agreement with the data of other authors. Thus, Brix et al [14] obtained for the integral cross section of the  $O^{16}(\gamma, n)O^{15}$  reaction (to 33 MeV) the value  $\sigma_0(\gamma, n) = 64 \pm 8$  MeV-mb. The integral cross section for the  $O^{16}(\gamma, p)N^{15}$  reaction for energies up to 30 MeV was estimated in the survey by Fuller and Hayward; [19] After adding up and combining the results of a number of authors [5,6,8,15] who had investigated the photoproton energy spectra by the emulsion technique, they obtained  $\sigma_0(\gamma, p) = 111$  MeV-mb.

It is seen from Table III (2) that 20% of the integral cross sections for reactions accompanied by the emission of one nucleon are associated with excitation energies greater than 30 MeV.

According to the theoretical investigations of the photodisintegration of oxygen, [1,2] all single-particle electric dipole transitions in  $O^{16}$  are associated with excitation energies below 30 MeV, and their integral cross section coincides with the integral cross section for the electric dipole absorption of photons by the oxygen nucleus. In connection with this conclusion of the theory, it is of interest to compare the theoretical value of the integral cross section for the electric dipole absorption of photons by an oxygen nucleus with the experimental value of the integral absorption cross section and also with the experimental value of the absorption cross section integrated over an excitation energy up to 30 MeV.

According to the summation rule, [25] the integral cross section for electric dipole absorption in the case of oxygen is

$$\sigma_0 = \frac{2\pi^2 e^2 \hbar}{Mc} \frac{NZ}{A} (1 + 0.8x) = 336 \text{ MeV} \cdot \text{mb}$$

(where the fraction of exchange forces is  $x = 0.5$ ). The experimental value of the integral cross section for the absorption of photons by oxygen nuclei estimated from the absolute yields for all photoneuclear reactions [21] is

$$\sigma_0 = 440 \text{ MeV} \cdot \text{mb}$$

We can obtain a more accurate value of the integral cross section if we use in the calculation of  $\sigma_0$  the value of the integral cross sections for the  $(\gamma, p)$  and  $(\gamma, n)$  reactions found not from the yields of these reactions but directly from the cross section curves taking into account transitions to excited states of the final nuclei (Table III, 2). This leads to an integral absorption cross section

$$\sigma_0 = 410 \text{ MeV} \cdot \text{mb}$$

Table IV

Reaction	Integral cross section, MeV-mb	
	$E_\gamma \leq 30$ MeV	$E_\gamma \leq 170$ MeV
$(\gamma, p)$	$100 \pm 4^{***}$	$117 \pm 5$
$(\gamma, n)$	$65 \pm 2$	$86 \pm 3$
$(\gamma, pn)^*$	$9 \pm 1$	$60 \pm 5$
$(\gamma, \alpha)$	4	4
$(\gamma, 4\alpha)$	5	5
Remaining reactions	(18)	$136_{-16}^{+0}$
Integral cross section for photon absorption	183 (201)**	$408_{-20}^{+10}$
$\int_0^{30} \sigma_{\text{abs}} dE$		
$\int_0^{170} \sigma_{\text{abs}} dE, \%$	45 (50)	100

\*The integral cross section for the  $(\gamma, pn)$  reaction was calculated directly from the cross section for this reaction.

\*\*Shown in the parenthesis is the upper limit for the cross section in which the approximate cross sections for the remaining photoneuclear reactions were taken into account.

\*\*\*The errors connected with the determination of the absolute irradiation intensity are not shown in the table; they are  $\sim 8\%$ .

With allowance for the uncertainty in the experimental and theoretical<sup>2)</sup> estimates of the value of the integral cross section, the two values seem to be in satisfactory agreement with one another. This allows us to state that the basic contribution to the integral absorption cross section comes from the electric dipole transitions, while, in any case, the magnetic dipole and electric quadrupole transitions do not exceed 20%.

We obtain the lower limit of the integral cross section for photon absorption in the excitation energy region below 30 MeV by summing the integral cross sections for the  $(\gamma, p)$ ,  $(\gamma, n)$ , and  $(\gamma, pn)$  reactions at energies up to 30 MeV and the cross sections for the  $(\gamma, \alpha)$  and  $(\gamma, 4\alpha)$  reactions from the data of [21]. We find the upper limit by taking into account the clear overestimation of the contribution from the  $(\gamma, p\alpha)$ ,  $(\gamma, \alpha n)$ , and  $(\gamma, 2p)$  reactions in the integral cross section for the absorption of photons of energy up to 30 MeV. The results of these estimates are shown in Table IV. It is seen from the table that the integral absorption cross section in the region of the giant resonance ( $E_\gamma < 30$  MeV) does not exceed 200 MeV-mb, i.e., it is 50–60% of the value expected from the calculations of Elliot and Flowers, [1] in which only the single-particle transi-

<sup>2)</sup>Rand, [26] using a shell model with a velocity-dependent potential, obtained an integral cross section that was 30% higher.

tions<sup>3)</sup> were taken into account. This difference between experiment and the theory based on the shell model is probably connected with the neglect of the strong correlations between the nucleons in the nucleus. As has been shown by Khlokhlov,<sup>[27]</sup> Levinger,<sup>[28]</sup> and Shklyarevskii,<sup>[29,30]</sup> the correlations between nucleons due to strong pairing interactions at small distances play a large role in the photoeffect in the high-energy region. These correlations make it possible to explain the emission of single photoprotons of energy up to 100 MeV from the nucleus, while the shell model yield for these particles is one-tenth as great.<sup>[30]</sup>

Thus, if the giant resonance is connected with resonance single-particle electric dipole transitions, we can state that the integral cross section for these transitions is 50–60% of the integral cross section for the electric dipole absorption of photons. The other half of the integral cross section for E1 absorption is associated with transitions in which strong correlations between nucleons at small distances play a role.

These correlations are probably very important even in  $(\gamma, p)$  and  $(\gamma, n)$  reactions accompanied by the emission of single nucleons from the nucleus. In fact, since the contribution of the M1 and E2 transitions to the integral absorption cross section is small,<sup>4)</sup> while the basic single-particle transitions are localized at excitation energies below 30 MeV, then the large integral cross section for the  $(\gamma, p)$  and  $(\gamma, n)$  reactions at energies above 30 MeV should be ascribed to transitions in which the correlations between nucleons are important.

It is further seen from Table IV that the  $(\gamma, p)$  and  $(\gamma, n)$  reactions accompanied by the emission of one nucleon from the nucleus are basic photonuclear reactions in oxygen. Their integral cross section is 50% of the integral cross section for photon absorption and their yield is 70% of the yield of all photonuclear reactions in oxygen.

Gell-Mann and Telegdi<sup>[32]</sup> have shown that if the nuclear forces are charge independent, then the cross sections and angular distributions of the  $(\gamma, p)$  and  $(\gamma, n)$  reactions should be the same for

<sup>3)</sup>A similar result was obtained recently by Burgov et al.<sup>[31]</sup> who measured the integral absorption cross section up to 26 MeV by the total absorption method and found that  $\sigma_0 = 149$  MeV-mb, in good agreement with our data for 26 MeV.

<sup>4)</sup>Consideration of the proton angular distributions in the  $(\gamma, p)$  reaction leads to the conclusion that the contribution from E2 transitions in the excitation region above the giant resonance is 5–10%.

identical final states (if we disregard interference effects). Taking into account the different thresholds and also corrections for the traversal of the potential barrier by neutrons and protons,<sup>[6]</sup> we find that the expected ratio of the integral cross sections for the  $(\gamma, n)$  and  $(\gamma, p)$  reactions decreases somewhat, while the value of this ratio depends on the angular momentum of the emitted particle.

It is seen from Table IV that the integral cross sections of the  $(\gamma, p)$  and  $(\gamma, n)$  reactions actually differ little:

$$\sigma_0(\gamma, n) / \sigma_0(\gamma, p) = 0.74 \pm 0.04.$$

2. Angular distributions of the  $(\gamma, p)$  and  $(\gamma, n)$  reactions. Since in the present work the states of the final  $N^{15}$  and  $O^{15}$  nuclei were not fixed, a detailed analysis of the experimental distributions cannot be made. Hence, we shall only comment on some special features of the resulting distributions.

As seen from Table II, for excitation energies  $E_\gamma \sim 21$ –28 MeV, corresponding to the giant resonance region, the ratio of the coefficient B/A in the proton angular distribution ( $E_p = 9$ –15 MeV) is  $1.0 \pm 0.5$ , while the same ratio in the neutron angular distribution ( $E_n = 5$ –11 MeV) is  $0.6 \pm 0.3$ . As we go to higher excitation energies, the ratio B/A increases; for  $E_p > 15$  MeV and  $E_n > 11$  MeV, the values of B/A in the proton and neutron angular distributions are practically the same (1.1–1.2).

These results can also be explained on the basis of the charge independence of nuclear forces if the different penetrability of the potential barrier for protons and neutrons emitted in the s and d states is taken into account. With an increase in the energy of the emitted nucleons, the difference in the penetrability of the barrier becomes unimportant and the ratio B/A for neutrons and protons becomes the same, as should be the case if nuclear forces are charge independent.

In the excitation energy region above the giant resonance, the ratio B/A  $\sim 1.2$  corresponds to a mixture of transitions with the emission of nucleons in the s and d states, as also follows from the theory; the nucleons are emitted in the d state in 70% of the cases.

Furthermore, it is seen from Figs. 3 and 4 that the maximum of the angular distribution for protons of energy  $E_p = 9$ –15 MeV is shifted in the forward direction to an angle  $\sim 70^\circ$ , while the angular distribution for neutrons of energy  $E_n = 5$ –11 MeV is symmetric relative to  $90^\circ$ . This result shows that at excitation energies corre-

sponding to the giant resonance, the electric quadrupole transitions give a certain contribution to the  $(\gamma, p)$  reaction cross section, but do not affect the  $(\gamma, n)$  cross section. The interference between the E1 and E2 transitions shifts the maximum of the proton angular distribution in the forward direction. The absence of an asymmetry in the neutron angular distribution in the giant resonance region is explained by the fact that the neutron cannot take part in single-particle E2 transitions, since its effective quadrupole charge is close to zero.

For  $E > 11$  MeV, however, it is seen from Fig. 4 that at excitation energies above the giant resonance the angular distributions of neutrons emitted in the  $O^{16}(\gamma, n)O^{15}$  reaction are also asymmetric. As was shown in 1959 in the thesis of V. A. Osipova, this asymmetry begins to appear for neutron energies  $E_n > 8$  MeV ( $E_\gamma > 24$  MeV). For neutron energies  $E_n > 11$  MeV ( $E_\gamma > 27$  MeV), the asymmetry is quite distinct. It is seen from Figs. 3 and 4 that the angular distributions of protons and neutrons emitted from the  $(\gamma, p)$  and  $(\gamma, n)$  reactions at excitation energies above 27–28 MeV have practically the same shape. In both distributions, the maximum is shifted forward to an angle  $\theta_{lab} \sim 70^\circ$ .

The fact that the maximum of the angular distribution for photoneutrons emitted from light and heavy elements is shifted forward has also been observed in a number of other experiments<sup>[15,33,34]</sup> in which the total yield of neutrons from different photonuclear reactions was recorded. Denisov et al<sup>[35]</sup> observed an asymmetry in the emission of neutrons produced in the  $C^{12}(\gamma, n)C^{11}$  reaction.

We have already noted that the asymmetry of the neutron angular distribution, comparable to the asymmetry of the proton angular distribution, is difficult to explain within the framework of the shell model. If we take into account transitions in which correlations between nucleons play an important role, then, as shown by Shklyarevskii,<sup>[30]</sup> it is possible to explain the large forward shift of the neutron angular distribution in the  $(\gamma, n)$  reaction.

## CONCLUSIONS

1. The integral cross section for the absorption of photons by oxygen nuclei computed up to an energy 170 MeV is in satisfactory agreement with the integral cross section for electric dipole absorption found with the aid of the summation rule. This allows us to state that the contribution of the electric quadrupole and magnetic dipole transitions to the integral absorption cross section is, in any case, no greater than 20%.

2. The integral cross section for single-particle E1 transitions, whose basic part, according to Elliot and Flowers, is localized in the excitation energy region below 30 MeV is only 50–60% of the dipole sum. The other half of the dipole sum is associated with transitions at higher energies in which strong correlations between nucleons are of importance.

3. The correlations between nucleons prove to be important not only for the photonuclear reactions in which several nucleons are emitted, but also for the  $(\gamma, p)$  and  $(\gamma, n)$  reactions in which one nucleon is emitted.

4. Comparison of the cross sections and angular distributions of the  $(\gamma, p)$  and  $(\gamma, n)$  reactions provides evidence in favor of the charge independence of nuclear forces.

5. At excitation energies above the giant resonance ( $E > 28$  MeV), the neutron angular distribution for the  $(\gamma, n)$  reaction is shifted in the forward direction. This asymmetry also leads to the conclusion that correlations between nucleons in the nucleus play an important role.

In conclusion, the authors express their gratitude to V. A. Dubrovina, A. I. Orlova, V. A. Sakovich, and V. S. Silaeva for taking part in the experiment and in the reduction of the experimental data.

<sup>1</sup>J. P. Elliot and B. H. Flowers, Proc. Roy. Soc. (London) **A242**, 57 (1957).

<sup>2</sup>Brown, Castillejo, and Evans, Nuclear Phys. **22**, 1 (1961).

<sup>3</sup>Balashov, Shevchenko, and Judin, Nuclear Phys. **27**, 323 (1961).

<sup>4</sup>D. L. Livesey, Can. J. Phys. **34**, 1022 (1956).

<sup>5</sup>Cohen, Mann, Patton, Reibel, Stephens, and Winhold, Phys. Rev. **104**, 108 (1956); Stephens, Mann, Patton, and Winhold, *ibid.* **98**, 839 (1955).

<sup>6</sup>S. A. E. Johansson and B. Forkman, Arkiv. Fysik **12**, 359 (1957).

<sup>7</sup>Milone, Milone-Tamburino, Rinzi, and Rubbino, Nuovo cimento **7**, 729 (1958).

<sup>8</sup>P. Brix and E. K. Maschke, Z. Physik **155**, 109 (1959).

<sup>9</sup>E. Finckh and U. Hegel, Z. Physik **162**, 154 (1961).

<sup>10</sup>A. S. Penfold and B. M. Spicer, Phys. Rev. **100**, 1377 (1955).

<sup>11</sup>J. H. Carver and K. H. Lokan, Australian J. Phys. **10**, 312 (1957).

<sup>12</sup>B. M. Spicer, Australian J. Phys. **10**, 326 (1957).

<sup>13</sup>H. King and L. Katz, Can. J. Phys. **37**, 1357 (1959).

- <sup>14</sup> Brix, Fuchs, Lindenberger, and Salander, *Z. Physik* **165**, 485 (1961).
- <sup>15</sup> C. Milone and A. Rubbino, *Nuovo cimento* **13**, 1035 (1959).
- <sup>16</sup> D. B. Isabelle and G. R. Bishop, LAL-1017 Laboratoire de l'Accelérateur lineaire, Orsay (1961).
- <sup>17</sup> Cohen, Fisher, and Warburton, *Phys. Rev.* **121**, 858 (1961).
- <sup>18</sup> Tanner, Thomas, and Meierhof, *Nuovo cimento* **14**, 257 (1959).
- <sup>19</sup> E. G. Fuller and E. Hayward, *Nuclear Reactions 2*, North Holland Publishing Company, 1962.
- <sup>20</sup> Gerasimov, Gorbunov, Ivanov, Kutsenko, and Spiridonov *PTÉ*, No. 3, 10 (1957).
- <sup>21</sup> Gorbunov, Dubrovina, Osipova, Silaeva, and Cerenkov, *JETP* **42**, 747 (1962), *Soviet Phys. JETP* **15**, 520 (1962).
- <sup>22</sup> P. M. S. Blackett and D. S. Lees, *Proc. Roy. Soc. (London)* **A134**, 658 (1932).
- <sup>23</sup> A. N. Gorbunov and V. M. Spiridonov, *JETP* **33**, 21 (1957), *Soviet Phys. JETP* **6**, 16 (1962).
- <sup>24</sup> D. H. Wilkinson, *Physica* **22**, 1039 (1956).
- <sup>25</sup> J. S. Levinger and H. A. Bethe, *Phys. Rev.* **78**, 115 (1950).
- <sup>26</sup> S. Rand, *Phys. Rev.* **107**, 208 (1957).
- <sup>27</sup> Yu. K. Khokhlov, *JETP* **23**, 241 (1952).
- <sup>28</sup> J. S. Levinger, *Phys. Rev.* **84**, 43 (1951).
- <sup>29</sup> G. M. Shklyarevskii, *JETP* **41**, 234 (1961), *Soviet Phys. JETP* **14**, 170 (1961).
- <sup>30</sup> G. M. Shklyarevskii, *JETP* **41**, 451 (1961), *Soviet Phys. JETP* **14**, 324 (1961).
- <sup>31</sup> Burgov, Danilyan, Dolbilkin, Lazareva, and Nikolaev, *JETP* **43**, in press, *Soviet Phys. JETP* **16**, in press.
- <sup>32</sup> M. Gell-Mann and V. L. Telegdi, *Phys. Rev.* **91**, 169 (1953).
- <sup>33</sup> L. A. Kul'chitskii and B. Presperin, *JETP* **37**, 1524 (1959), *Soviet Phys. JETP* **10**, 1082 (1960).
- <sup>34</sup> G. C. Reinhardt and W. D. Whitehead, *Nuclear Phys.* **30**, 201 (1962).
- <sup>35</sup> Denisov, Kosareva, Tel'nov, and Cerenkov, *Tr. II Vsesoyuznoi konferentsii po yadernym reaktsiyam pri malykh and srednikh energiakh* (Proc. of the Second All-Union Conf. on Nuclear Reactions at Low and Medium Energies) (in press).

Translated by E. Marquit